AGU PUBLICATIONS

Paleoceanography

RESEARCH ARTICLE
10.1002/2016PA002932

Pacific-Atlantic Circumpolar Deep Water coupling during the last 500 ka

Johannes Ullermann[1], Frank Lamy[1], Ulysses Ninnemann[2], Lester Lembke-Jene[1], Rainer Gersonde[1], and Ralf Tiedemann[1]

[1]Alfred-Wegener-Institut Helmholtz-Zentrum für Polar- und Meeresforschung, Bremerhaven, Germany, [2]Department of Earth Science and Bjerknes Centre of Climate Research, University of Bergen, Bergen, Norway

Key Points:
- Continuous Pacific-Antarctic circumpolar deepwater mass exchange throughout the past 500 ka
- A common circumpolar deepwater mass was maintained between the SE Pacific and the SE Atlantic (Northern Cape Basin)
- Deep waters in the southernmost SE Atlantic evolved differently from a common water mass in the SE Pacific and the SE Atlantic

Supporting Information:
- Supporting Information S1

Correspondence to:
F. Lamy,
Frank.Lamy@awi.de

Citation:
Ullermann, J., F. Lamy, U. Ninnemann, L. Lembke-Jene, R. Gersonde, and R. Tiedemann (2016), Pacific-Atlantic Circumpolar Deep Water coupling during the last 500 ka, *Paleoceanography*, *31*, 639–650, doi:10.1002/2016PA002932.

Received 5 FEB 2016
Accepted 17 MAY 2016
Accepted article online 20 MAY 2016
Published online 11 JUN 2016

Abstract Investigating the interbasin deepwater exchange between the Pacific and Atlantic Oceans over glacial-interglacial climate cycles is important for understanding circum-Antarctic Southern Ocean circulation changes and their impact on the global Meridional Overturning Circulation. We use benthic foraminiferal $\delta^{13}C$ records from the southern East Pacific Rise to characterize the $\delta^{13}C$ composition of Circumpolar Deep Water in the South Pacific, prior to its transit through the Drake Passage into the South Atlantic. A comparison with published South Atlantic deepwater records from the northern Cape Basin suggests a continuous water mass exchange throughout the past 500 ka. Almost identical glacial-interglacial $\delta^{13}C$ variations imply a common deepwater evolution in both basins suggesting persistent Circumpolar Deep Water exchange and homogenization. By contrast, deeper abyssal waters occupying the more southern Cape Basin and the southernmost South Atlantic have lower $\delta^{13}C$ values during most, but not all, stadial periods. We conclude that these values represent the influence of a more southern water mass, perhaps Antarctic Bottom Water (AABW). During many interglacials and some glacial periods, the gradient between Circumpolar Deep Water and the deeper southern Cape Basin bottom water disappears suggesting either no presence of AABW or indistinguishable $\delta^{13}C$ values of both water masses.

1. Introduction

Benthic foraminiferal $\delta^{13}C$-based studies in the Southern Ocean have largely focused on the South Atlantic, because the region is an important intersection point of major deepwater masses and thus crucial for understanding the role of the oceans' physical circulation during glacial-interglacial climate change, particularly with regard to the carbon cycle. At this critical junction, North Atlantic Deep Water (NADW) and Weddell Sea-derived Antarctic Bottom Water (W-AABW) mix with Circumpolar Deep Water (CDW), which is inflowing from the South Pacific. In this respect, a quantified understanding of past tracer distributions in the Atlantic basin is immanently important to infer potential changes in physical ocean circulation, which may have influenced the oceans capacity in sequestering atmospheric CO_2 at depth [e.g., *Gebbie*, 2014; *Hesse et al.*, 2011; *Hoffman and Lund*, 2012; *Lund et al.*, 2011; *Wunsch*, 2003].

So far, past $\delta^{13}C$ changes of Pacific CDW, prior to its transition trough the Drake Passage into the Atlantic, have been less well constrained and remain largely uncertain. Only few benthic foraminiferal $\delta^{13}C$-based studies have attempted to define the CDW $\delta^{13}C$ composition from the Southeast Pacific (SE Pacific) and discussed the interbasin coupling to the Southeast Atlantic (SE Atlantic) [*Hodell et al.*, 2000; *Matsumoto and Lynch-Stieglitz*, 1999; *Ninnemann and Charles*, 2002]. *Ninnemann and Charles* [2002] revealed that an interbasin $\delta^{13}C$ gradient of ~0.6‰ developed between the East Pacific Rise and the deep southern Cape Basin during the Last Glacial Maximum (LGM). In contrast, the modern eastward advection of CDW continuously homogenizes the deepwater properties between both areas [*Orsi et al.*, 1999, 2002; *Reid*, 1986, 1989], with nearly no interbasin $\delta^{13}C$ gradient [*Kroopnick*, 1985]. The reconstructed glacial interbasin $\delta^{13}C$ difference originated from a much higher $\delta^{13}C$ decrease of the deep waters occupying the southern Cape Basin and adjoining southernmost South Atlantic areas than those occupying the East Pacific Rise [*Curry and Oppo*, 2005; *Mackensen et al.*, 2001; *Martínez-Méndez et al.*, 2009; *Ninnemann and Charles*, 2002]. Accordingly, past $\delta^{13}C$ of bottom water was diverging in the Pacific and Atlantic, indicating a fundamentally altered deepwater exchange and increased bottom water heterogeneity between the basins during the LGM. This reconfiguration was accompanied by changes in the formation mode of W-AABW or its glacial equivalent [*Ninnemann and Charles*, 2002], which had a low end-member $\delta^{13}C$ signature [*Curry and

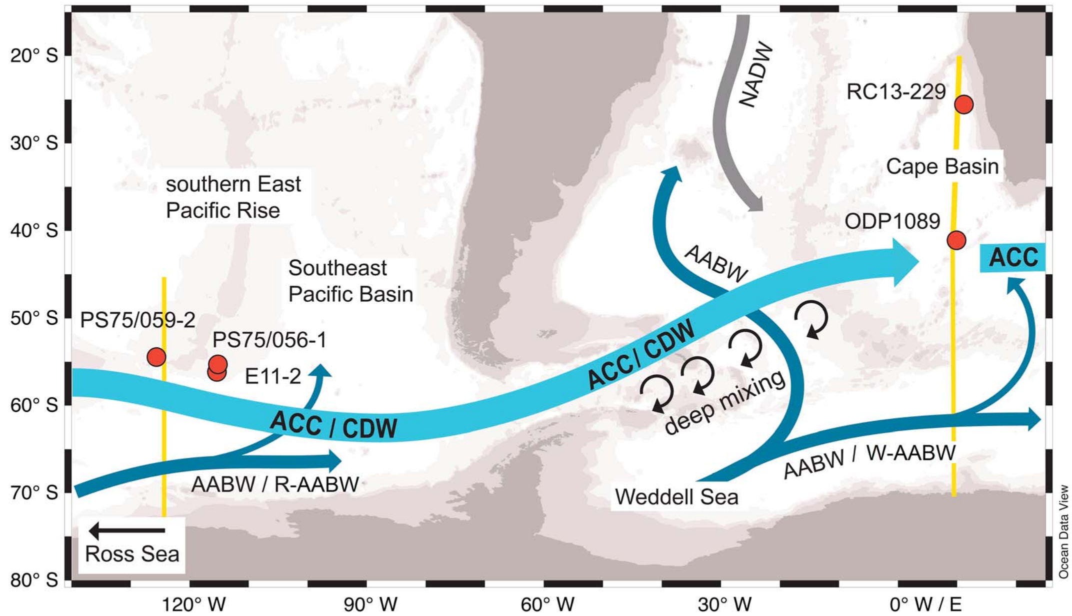

Figure 1. Map showing positions of discussed cores in the context of the modern deepwater hydrography; ocean and land topography is from Ocean Data View (ODV) [*Schlitzer*, 2012]; circles indicate position of cores discussed in this study; arrows show schematic flow path of major deepwater masses (CDW, Circumpolar Deep Water; AABW, Antarctic Bottom Water; NADW, North Atlantic Deep Water); two subtypes of AABW are indicated (R-AABW, Ross Sea derived AABW; W-AABW, Weddell Sea derived AABW); positions of the hydrographic sections displayed in Figure 2 are indicated as yellow lines.

Oppo, 2005]. However, this inference about the deepwater exchange between the Pacific and Atlantic basins is basically restricted to the last glacial-interglacial cycle and based on the benthic $\delta^{13}C$ record of only a single core (E11-2) [*Ninnemann and Charles*, 2002] to define the Pacific CDW changes. Core E11-2 was retrieved from ~3000 m water depth, close to the core layer of southward flowing Pacific Deep Water (PDW). Potential changes in the influence of this deepwater mass may therefore have influenced the Pacific CDW record [*Ninnemann and Charles*, 2002]. Thus, it is difficult to assess to what extent this interbasinal decoupling is an intrinsic characteristic of late Pliestocene glaciations, confounding our understanding of which Southern Ocean water mass and with what composition fed the glacial abyss.

Changes in physical ocean circulation likely accounted for a large portion of the ~90 ppmv decline in atmospheric CO_2 concentrations, which occurred during each of the last five glaciations [*Lüthi et al.*, 2008; *Petit et al.*, 1999]. Concepts that invoke atmospheric CO_2 storage in the deep ocean [*Adkins*, 2013; *Toggweiler*, 1999], particularly in the Atlantic interior [*Skinner*, 2009], rely on the observation that the LGM distribution of $\delta^{13}C$ in the Atlantic displayed a higher vertical gradient than today at middepth, thus indicating a much stronger intermediate to deep ocean chemical stratification [*Curry and Oppo*, 2005; *Curry et al.*, 1988; *Duplessy et al.*, 1988; *Hoffman and Lund*, 2012; *Ninnemann and Charles*, 2002]. Accordingly, the LGM distribution of $\delta^{13}C$ may imply less mixing of glacial-AABW (low-$\delta^{13}C$) and glacial-NADW (high-$\delta^{13}C$), which, in essence, would increase the deep oceans ability to sequester atmospheric CO_2. In this regard, a quantified understanding of the LGM $\delta^{13}C$ distribution in the Atlantic is important. Particularly, the occurrence of the extremely low $\delta^{13}C$ values in the southernmost South Atlantic is critical, as they provide indications on the LGM end-member $\delta^{13}C$ signature of AABW [*Curry and Oppo*, 2005; *Marchitto and Broecker*, 2006], which is a basic parameter for ocean modeling and proxy-based numerical calculations [e.g., *Gebbie*, 2014; *Hoffman and Lund*, 2012]. In addition, it is important to characterize Pacific CDW changes for understanding glacial-interglacial atmospheric CO_2 cycles, since stronger ocean chemical stratification in the Atlantic was a persistently recurring pattern [*Hodell et al.*, 2003a].

In this study, we extend and improve the temporal resolution of the currently sparse Pacific CDW record by presenting two new, benthic foraminiferal $\delta^{13}C$ records (PS75/059-2 and PS75/056-1) from the SE Pacific that

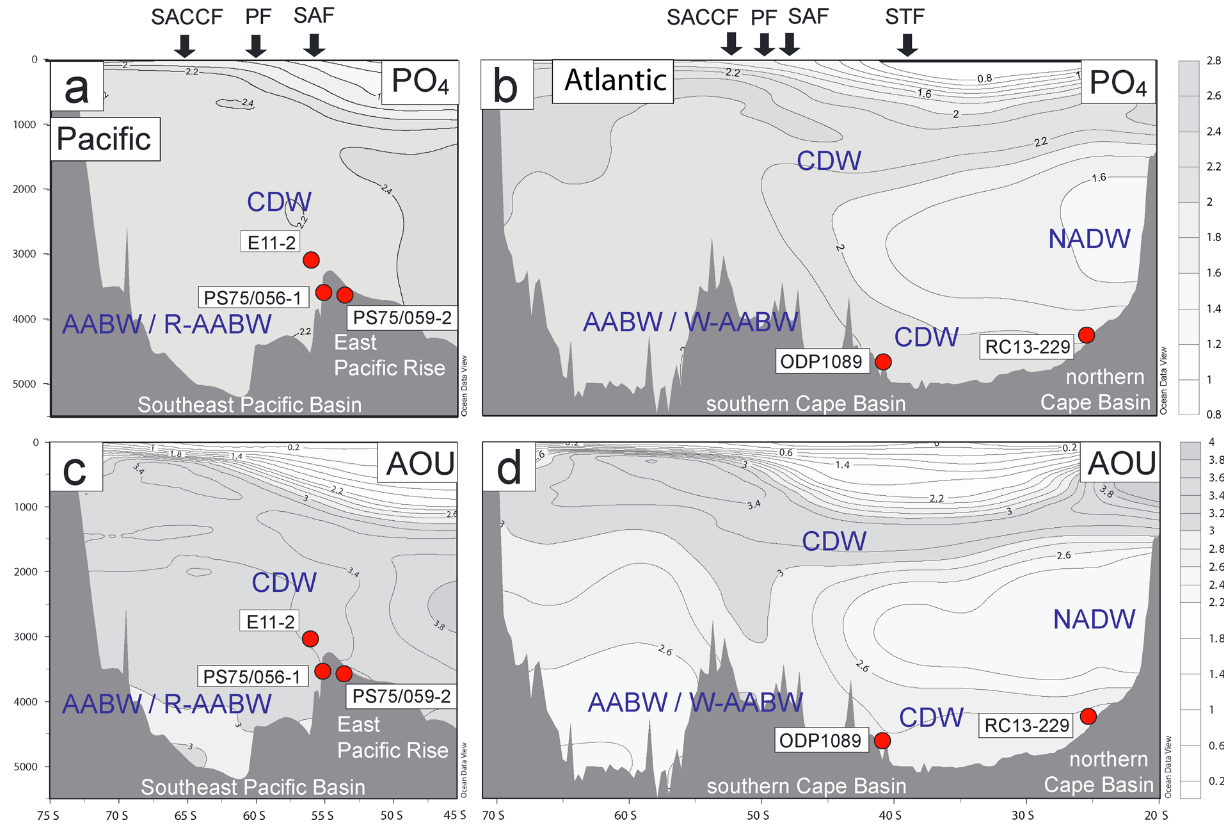

Figure 2. Modern $\delta^{13}C$ (PO_4^{3-} derived) and AOU distribution for (a and c) the Southeast Pacific and (b and d) the Southwest Atlantic; the position of sections are indicated in Figure 1 as yellow lines; the [PO_4^{2-}] and AOU are from the WOA09 (gridded) data compilation [*Garcia et al.*, 2010a, 2010b]; for data visualization Ocean Data View (ODV) was used [*Schlitzer*, 2012]; circles indicate positions of cores discussed in this study; surface positions of Southern Ocean fronts are marked by arrows (STF, Subtropical Front; SAF, Subantarctic Front; PF, Polar Front; SACCF, Southern ACC Front), according *Orsi et al.* [1995]; Southern Ocean deepwater masses are indicated (CDW, Circumpolar Deep Water; AABW, Antarctic Bottom Water; NADW, North Atlantic Deep Water); two subtypes of AABW are indicated (R-AABW, Ross Sea derived AABW; W-AABW, Weddell Sea derived AABW).

were recovered from the southern East Pacific Rise, within the core CDW layer, about 500 m deeper than the existing reference record E11-2 [*Ninnemann and Charles*, 2002]. We discuss the interbasin link to the SE Atlantic and its implications on atmospheric CO_2 storage over the past 500 ka by comparing our results to published records from sites in the abyssal northern (RC13-229; ~4200 m water depth [*Oppo and Fairbanks*, 1987; *Oppo et al.*, 1990]) and southern Cape Basin (Ocean Drilling Program (ODP) Site 1089;~4600 m water depth [*Hodell et al.*, 2001, 2003b]). The former core stems from a more northern latitudinal position than the ones considered in previous LGM interbasin comparisons [*Ninnemann and Charles*, 2002]. Today, both Cape Basin sites are bathed in CDW, but well located to detect Atlantic-internal changes of past AABW export.

2. Modern Deep Water Circulation

All core sites in this study are presently bathed in CDW (Figures 1 and 2), which forms through mixing with northern and southern-sourced deepwater masses as it flows eastward within the Antarctic Circumpolar Current (ACC) [*Broecker et al.*, 1998; *Johnson*, 2008]. In the SE Pacific, Ross Sea-generated Antarctic Bottom Water (R-AABW) spreads into the SE Pacific Basin at abyssal depths, without directly influencing the shallower core sites on the East Pacific Rise [*Orsi et al.*, 1999; *Pardo et al.*, 2012]. The principal source of the deep water that fills the Cape Basin today is Pacific CDW, which enters the South Atlantic basin through the Drake Passage [*Orsi et al.*, 1999; *Reid*, 1989]. However, unlike in the SE Pacific, the core sites in the SE Atlantic are additionally influenced by NADW and W-AABW. Their incorporation into CDW is enhanced by turbulent mixing over rough topography in the Scotia Sea, immediately after CDW has entered the South Atlantic through the Drake Passage [*Naveira Garabato et al.*, 2002, 2007; *Orsi et al.*, 1999]. Thus, the South Atlantic CDW composition gradually becomes modified.

The $\delta^{13}C$ of dissolved inorganic carbon ($\delta^{13}C_{DIC}$) in seawater is a nonconservative tracer, as its modern distribution in the deep ocean depends, besides water mass mixing, mainly on biological cycling. Further, isotopic fractionation during air-sea gas exchange has a contributing influence on seawater $\delta^{13}C_{DIC}$ [e.g., *Lynch-Stieglitz*, 2003]. Today, it is largely linearly related to seawater nutrient concentrations, e.g., to phosphate concentrations [*Kroopnick*, 1985]. Figures 2a and 2b show the [PO_4^{3-}] concentration in seawater from two north-south sections at longitudes of the SE Pacific and SE Atlantic core sites (WOA09 (gridded) data compilation [*Garcia et al.*, 2010a]). In the SE Pacific, the [PO_4^{3-}] concentrations in CDW at the core sites are rather uniformly distributed, accordingly the core sites feature a similar $\delta^{13}C$ signature (Table S1). In the SE Atlantic, the low [PO_4^{3-}] (high $\delta^{13}C_{DIC}$) values between 2000 m and 3500 m are due to the intrusion of NADW, separating CDW into an upper and lower layers. After passing through the Drake Passage, CDW also interacts with W-AABW (high [PO_4^{3-}]/low-$\delta^{13}C_{DIC}$) at its base [*Orsi et al.*, 1999]. In addition, a north-south gradient exists across the SE Atlantic at these depths due to continuously increasing contributions of AABW toward Antarctica [*Broecker et al.*, 1998; *Johnson*, 2008]. In the Cape Basin, the regional north-south gradient in [PO_4^{3-}] concentrations is relatively small (Figure 2).

The apparent oxygen utilization (AOU) distribution (WOA09 (gridded) data compilation [*Garcia et al.*, 2010b]) further illustrates the water mass distribution in both basins (Figures 2c and 2d). For the SE Pacific section, the AOU shows that nearly homogenous CDW occupies wide areas, whereas R-AABW is restricted to the deep southeast Pacific basin. For the SE Atlantic section, the AOU clearly outlines CDW as a separate water mass, in addition to NADW and W-AABW. The high AOU signature on the East Pacific Rise can be traced to the northern and southern Cape Basin.

3. Material and Methods

3.1. Sample Material

Piston core PS75/059-2 (54°12.90′S 125°25.53′W; 3613 m water depth; 13.98 core length) and gravity core PS75/056-1 (55°09.74′S; 114°47.31′W; 3581 m water depth; 10.21 core length) were recovered during R/V *Polarstern* cruise ANT-XXVI/2 [*Gersonde*, 2011]. The sites are located on the western (PS75/059-2) and eastern (PS75/056-1) flank of the southern East Pacific Rise, immediately north of the Eltanin Fracture Zone (Figure 1).

3.2. Stable Isotopes

For oxygen and carbon isotope analyses the working halves of both cores were sampled in 1 cm thick slices at 5 cm intervals. After freeze drying, the samples were wet sieved over a 63 μm mesh size, rinsed with deionized water, and dried at a temperature under 40°C. Benthic foraminiferal species *Cibicidoides wuellerstorfi* and *Cibicidoides kullenbergi* were picked from the 250–400 μm size fraction. The stable isotope composition of one to six foraminifera tests was analyzed on a Finnigan MAT 251 or Finnigan MAT 253 isotope ratio mass spectrometer, each coupled with a Kiel Carbo (II, IV) carbonate preparation device, at the AWI Bremerhaven. Isotope ratios of $^{18}O/^{16}O$ and $^{13}C/^{12}C$ are expressed in the δ-notation versus Vienna Peedee belemnite (VPDB). The isotope measurements were calibrated to the VPDB scale using the international NIST 19 standard. The long-term precision of the measurements based on the repeated analyses of an internal laboratory carbonate standard (Solnhofen limestone) was better than ±0.08‰ for $\delta^{18}O$ and ±0.06‰ for $\delta^{13}C$. The samples of core PS75/059-2 were measured primarily on the Finnigan MAT 251 mass spectrometer, while PS75/056-1 samples were measured entirely on the Finnigan MAT 253 mass spectrometer. The benthic $\delta^{18}O$ data of core PS75/059-2 and core PS75/056-1 have been published previously [*Lamy et al.*, 2014]. For core PS75/059-2, isotope measurements were primarily carried out on monospecific samples of *C. kullenbergi*. Only in few cases, monospecific samples of *C. wuellerstorfi* and mixed specific samples were measured (Figure S1 in the supporting information). For core PS75/056-1, all measurements were carried out on monospecific samples of *C. kullenbergi.*

3.3. Age Model and Sedimentation Rates

The age models of cores PS75/059-2 and PS75/056-1 are based on the correlation of the benthic $\delta^{18}O$ records to the LR04 benthic $\delta^{18}O$ stack [*Lisiecki and Raymo*, 2005], using the Match software [*Lisiecki and Lisiecki*,

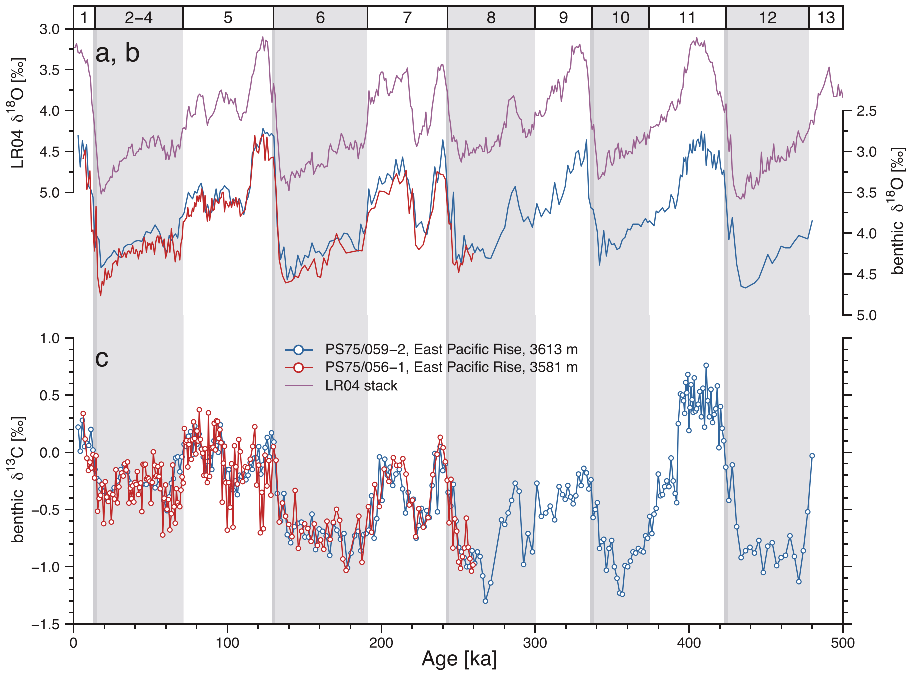

Figure 3. East Pacific Rise records from opposite ridge flanks. (a) LR04 benthic $\delta^{18}O$ stack for stratigraphic reference. (b) Benthic $\delta^{18}C$ records of cores PS75/059-2 and PS75/056-1. (c) Benthic $\delta^{13}C$ records of cores PS75/059-2 and PS75/056-1; areas shaded in grey highlight glacial intervals.

2002]. The $\delta^{18}O$ values between the two cores are consistent throughout the entire record and match well (Figure 3). However, a small constant offset of ~0.1‰ exists between the benthic foraminiferal $\delta^{18}O$ records of cores PS75/059-2 and PS75/056-1 (Figure 3). As the $\delta^{18}O$ signature of benthic foraminiferal tests vary as a function of ambient bottom water temperature and seawater $\delta^{18}O$ distribution [e.g., *Lynch-Stieglitz*, 2003], slight contrasts in these two water mass parameters may have been present across the East Pacific Rise. Today, cold Ross Sea-derived AABW flows down the Antarctic continental slope and fills the Eastern Pacific Basin at abyssal depth (Figures 1 and 2), approaching the East Pacific Rise from north and east [*Orsi et al.*, 1999, 2002], i.e., the side of the location of core site PS75/056-1. Based on inferences from benthic foraminiferal $\delta^{18}O$ based studies from the Atlantic [*Hoffman and Lund*, 2012; *Mackensen et al.*, 2001], the ~0.1‰ enriched benthic $\delta^{18}O$ values at core site PS75/056-1 may thus originate from a slightly higher influence of R-AABW at the of the southern East Pacific Rise throughout the past, which is not reflected in the respective benthic $\delta^{13}C$ records. However, we note that such a small offset is in principle within the range of interspecies variability in foraminifera.

For core PS/75-059-2 the resulting average sedimentation rate is ~3 cm/ka, with maxima reaching ~6 cm/ka during the interval between 390 ka and 420 ka (marine oxygen isotope stage (MIS) 11; Figure S2). This interval is characterized by higher coccolith contents and carbonate components, constituting nearly 100 wt % [*Gersonde*, 2011]. For core PS/75-056-1, the average sedimentation rate is ~6.0 cm/ka in the upper part (6–110 ka) and ~3.0 cm/ka further downcore (110–260 ka; Figure S2). For consistency, we re-tuned the published records of E11-2, RC13-229, ODP Site 1090 and ODP Site 1089 (Table S1 in the supporting information) to the LR04 benthic $\delta^{18}O$ stack (Figure S3).

4. Results and Discussion

4.1. East Pacific Rise: Pacific CDW Reference Locations

The $\delta^{13}C$ signature measured on tests of the benthic foraminiferal *C. wuellerstorfi* record the bottom water $\delta^{13}C$ composition in a one-to-one relationship [*Curry et al.*, 1988; *Duplessy et al.*, 1984, 1988]. Parallel

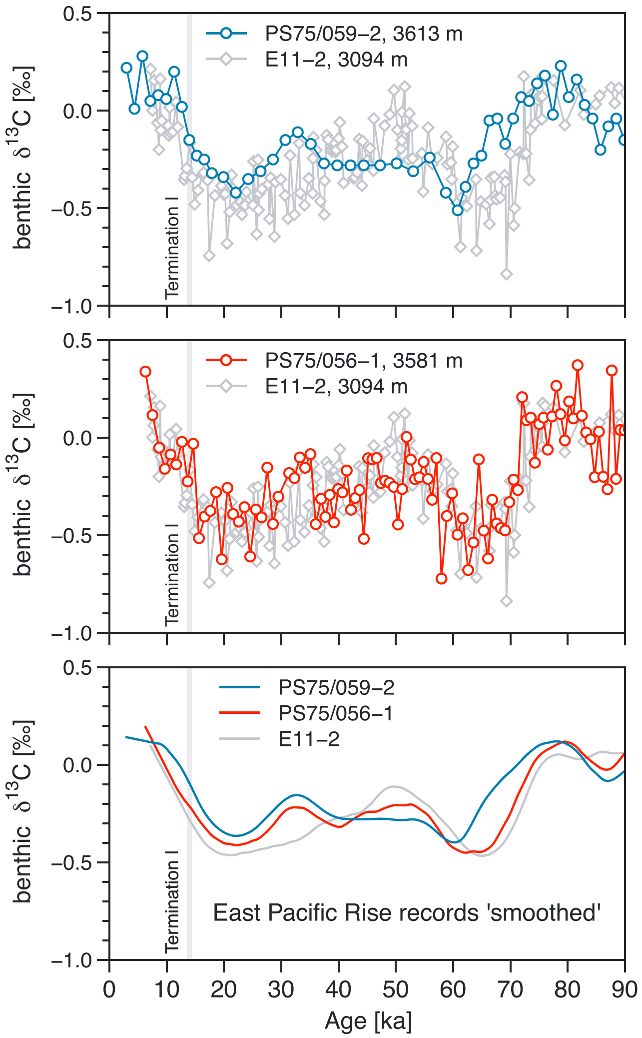

Figure 4. Comparison between benthic $\delta^{13}C$ records from the East Pacific Rise. (a) Records PS75/059-2 and E11-2. (b) Records PS75/056-1 and E11-2. (c) Smoothed time series of records PS75/059-2, PS75/056-1, and E11-2, calculated by kernel method; gray vertical line marks the last glacial termination.

measurements of the benthic foraminiferal *C. wuellerstorfi* and *C. kullenbergi* (or *C. mundulus*) from a midlatitude SE Pacific core off Chile reveal constant down-core deviations of ~0.16‰ between both species [*Martínez-Méndez et al.*, 2013]. Given that records PS75/059-2 and PS75/056-1 almost completely consist of monospecific samples of *C. kullenbergi* (Figure S1), we assume that their amplitude changes adequately reflect bottom water $\delta^{13}C$ compositional changes at the East Pacific Rise. Yet their absolute values could be about ~0.16‰ offset.

Core PS75/059-2 (3613 m water depth), recording past bottom water $\delta^{13}C$ composition at the western side of the East Pacific Rise, displays large glacial-interglacial variations over the last 480 ka, with amplitudes ranging between ~0.3‰ and ~1.5‰ at glacial terminations (Figure 3). Lowest values of −1.3‰ and −1.2‰ occur during MIS 8 and MIS 10, respectively, with an increasing long-term trend thereafter. The $\delta^{13}C$ record of core PS75/056-1 (3581 m water depth), from the eastern side of the East Pacific Rise, shows an almost perfect match on orbital time scales (Figure 3). This suggests that the topography of the intervening ridge crest had no significant influence on the local $\delta^{13}C$ distribution. Today, the $\delta^{13}C$ distribution at the East Pacific Rise, as derived from phosphate (Figure 2), is almost homogeneous in the water column below 1200 m. The match between our benthic $\delta^{13}C$ records of cores PS75/059-2 and PS75/056-1 indicates a likewise homogeneous distribution, at least across the last two glacial-interglacial cycles (Figure 3). Comparison of our records to the published $\delta^{13}C$ values of core E11-2 located ~500 m shallower (Figure 4; 3094 m water depth) validates the homogeneity of a substantial portion of SE Pacific CDW at orbital time scales.

Overall, our results imply that all three benthic $\delta^{13}C$ records are representative for an almost homogeneous water mass on glacial-interglacial timescales, which occupies the East Pacific Rise area over a larger depth range. We therefore name the water mass documented at the respective core locations as CDW, being aware that its $\delta^{13}C$ composition represents actually the lower portion of CDW (lower CDW). Referring to the previous study by *Ninnemann and Charles* [2002], our reconstructions from deeper cores extend the previous CDW reference record from core E11-2. However, on suborbital time scales transient differences of up to ~0.3‰ occur among the three records during parts of MIS 3 (Figure 4). Partly, these differences may result from their different sedimentation-rates and age model offsets. Alternatively, small suborbital variations in relative contributions of PDW versus SE Pacific CDW affected the shallower core site E11-2.

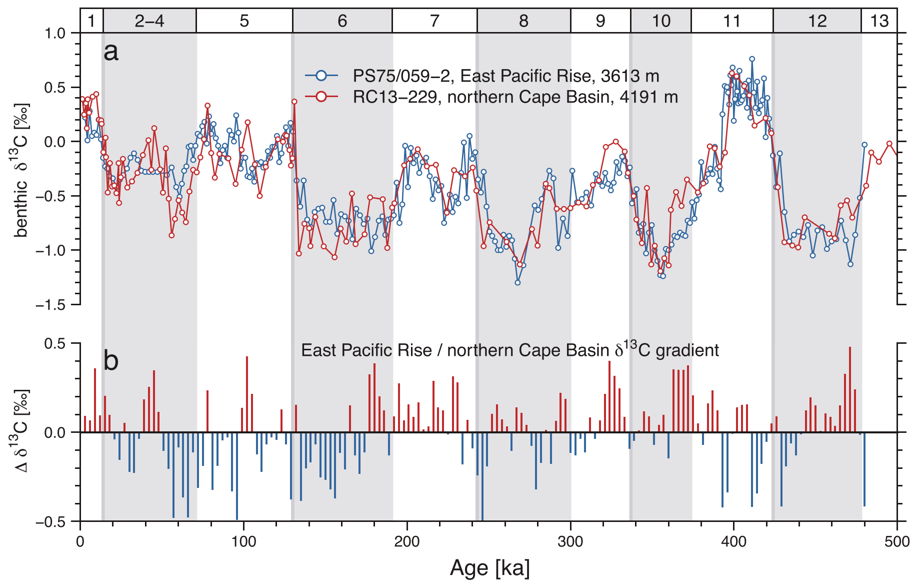

Figure 5. Comparison between East Pacific Rise and northern Cape Basin. (a) Benthic $\delta^{13}C$ records PS75/059-2 and RC13-229. (b) Difference between benthic $\delta^{13}C$ records PS75/059-2 and RC13-229 ($\Delta\delta^{13}C = \delta^{13}C_{RC13\text{-}229} - \delta^{13}C_{PS75/059\text{-}2}$); note that it shows any long-term trend; before subtraction the original time series were resampled in 3 ka spacing with linear interpolation between data points; areas shaded in grey highlight glacial intervals; for resampling the *AnalySeries* program was used [*Paillard et al.*, 1996].

4.2. Pacific-Atlantic Interbasin Link

Our East Pacific Rise records depict the $\delta^{13}C$ composition of SE Pacific CDW prior to its transition trough the Drake Passage and can thus be used as the Pacific end-member for interbasin deepwater exchange in the Southern Ocean. We therefore discuss the past Pacific CDW influence on SE Atlantic southern-sourced deep waters. We compare our results to the benthic $\delta^{13}C$ reference records from core RC13-229 and ODP Site 1089 located in the abyssal northern and southern Cape Basin, respectively (Figure 2). For the following discussion, we assume that $\delta^{13}C$ values in the southern Cape Basin (ODP Site 1089) and in the northern Cape Basin (RC13-229) reflect a water mass-controlled signal. However, it is under discussion whether the very depleted $\delta^{13}C$ values measured on benthic foraminifera species *C. wuellerstorfi* and *C. kullenbergi* from the southern Cape Basin reflect solely a water mass signal, or whether they might be in addition influenced by local, biological, or environmental factors [*Hodell et al.*, 2003a; *Mackensen et al.*, 1993; *Ninnemann and Charles*, 2002; *Piotrowski et al.*, 2005]. Indications for such impact in the southern Cape Basin are discontinuous, parallel isotope measurements on both foraminifera species at ODP Site 1090 in the southern Cape Basin (water depth ~3700 m). These data show higher $\delta^{13}C$ values for C. *wuellerstorfi* than for C. *kullenbergi* (Figure S4) [*Hodell et al.*, 2000, 2003a; *Venz and Hodell*, 2002] during MIS 2–4, whereas the values are similar during interglacials.

On orbital time scales, the benthic $\delta^{13}C$ records PS75/059-2 and RC13-229, which are based on benthic foraminiferal *C. wuellerstorfi* measurements, are virtually identical (Figure 5a), showing similar absolute values and down-core variability. The consistency of the records is corroborated by the absence of a long-term trend in the difference between both records (Figure 5b). This is consistent with the phosphate-derived modern seawater $\delta^{13}C$ difference of ~0.1‰ of the water masses overlying both core sites (Table S1).

On suborbital time scales, differences of up to 0.4‰ appear, especially in the past 150 kyr (Figure 5b), without significant glacial-interglacial pattern characteristics. Despite potential influences by differences in the temporal resolution of both records or age model uncertainties, this variability may indicate changes in ocean circulation, induced by a varying influence of local, northern and southern-sourced water masses in the SE Atlantic [*Piotrowski et al.*, 2005, 2008]. Nonetheless, if the benthic $\delta^{13}C$ record PS75/059-2 reliably reflects the evolution of past CDW composition at the East Pacific Rise, the comparison implies for orbital time scales that a common CDW composition was maintained for the Pacific and the Atlantic basin over the past 480 ka. In turn, this suggests a continuous coupling between CDW at the East Pacific Rise and in the northern Cape

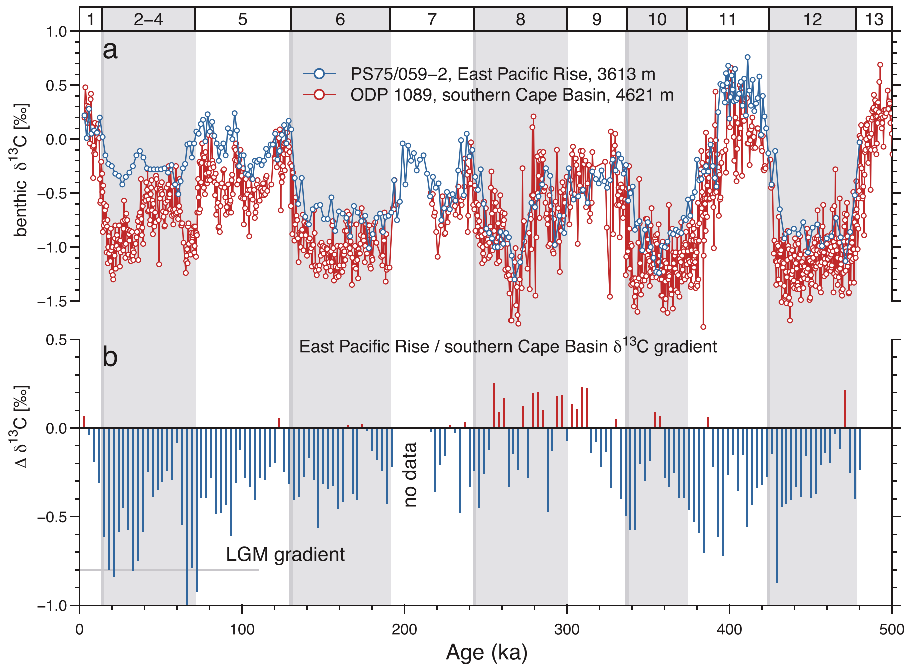

Figure 6. Comparison between East Pacific Rise and southern Cape Basin. (a) Benthic δ^{13}C records PS75/059-2 and ODP Site 1089. (b) Difference between benthic δ^{13}C records PS75/059-2 and ODP Site 1089 ($\Delta\delta^{13}C = \delta^{13}C_{ODP\ Site\ 1089} - \delta^{13}C_{PS75/059\text{-}2}$); the original time series ODP Site 1089 was smoothed using a 5-point moving average; before subtraction the smoothed time series ODP Site 1089 and the original time series PS75/059-2 were resampled in 3 ka spacing with linear interpolation between data points; the LGM gradient (~ −0.6‰) is an average of the values between 18 ka and 24 ka; areas shaded in grey highlight glacial intervals; for resampling and smoothing the *AnalySeries* program was used [*Paillard et al.*, 1996].

Basin, consistent with the notion that benthic δ^{13}C values of northern Cape Basin core RC13-229 reflect the δ^{13}C composition of average CDW [*Oppo et al.*, 1990].

Our C *kullenbergi* δ^{13}C records from South Pacific cores PS75/059-2 and PS75/056-1 are on orbital timescales similar to the southern Cape Basin C. *wuellerstorfi* data from ODP Site 1090 and and identical to the northern Cape Basin δ^{13}C record from core RC13-229, which consists of on C *wuellerstorfi* measurements only [*Oppo and Fairbanks*, 1987; *Oppo et al.*, 1990] (Figure S4). This indicates that influences by local, biological, or environmental factors were minor. Apparently, our predominantly used foraminiferal species C *kullenbergi* record the "true" water mass δ^{13}C composition, and thus the δ^{13}C evolution of South Pacific CDW.

It is important to note that in contrast to our results, former benthic δ^{13}C-based observations by *Ninnemann and Charles* [2002] implied a diverging δ^{13}C evolution for the SE Pacific and SE Atlantic area, associated with the development of a high interbasin δ^{13}C gradient of ~0.6‰ at the LGM. This interbasinal contrast arises when comparing to the deeper southern, and not to the northern Cape Basin records [*Ninnemann and Charles*, 2002]. Similar differences are visible, when comparing the East Pacific Rise record PS75/059-2 with the southern Cape Basin reference record ODP Site 1089 [*Hodell et al.*, 2001]. The ODP Site 1089 data show considerably lower δ^{13}C values over much of its length, particularly during the LGM (Figure 6). The difference between the East Pacific Rise—southern Cape Basin records, or interbasin δ^{13}C gradient, was highest during the last glacial cycle (MIS 2 and 4) with offsets of ~0.8‰. The gradient re-occurred, albeit with lower amplitude, several times over the past ~500 ka. Interbasinal gradients developed during glacial MIS 6, 10, and 12. However, the interbasin gradient displays an irregular, rather than systematic, glacial-interglacial modulation with gradients also apparent during interglacial MIS 11 (Figure 6), as well as with periods of absence, e.g., during late MIS 9 through MIS 8 and MIS 7. The fact that our LGM interbasin δ^{13}C gradient (~0.8‰) is ~0.2‰ higher than the originally reported one (~0.6‰) originates from relatively high glacial values of core PS75/059-2, when compared to E11-2 used previously [*Ninnemann and Charles*, 2002]. We conclude that the strength of the interbasin δ^{13}C gradient might not only or simply indicate the degree of deepwater decoupling between the SE Pacific and SE Atlantic. Rather, it portrays the independent evolution of deep waters that bathed the southern Cape Basin and adjoining southernmost South Atlantic areas, with regard to a common SE Pacific and SE Atlantic CDW evolution. In other words, it appears as if there is a continuously homogeneous CDW mass present in both basins with another deeper more southern water mass (perhaps AABW). During many interglacials (MIS 1, 5, 7, and 9) and some glacial periods (MIS 8, as well as portions of MIS 6 and 10), the gradient between CDW and the deeper southern Cape Basin bottom water disappears, suggesting either no presence of AABW or that CDW and AABW δ^{13}C values are indistinguishable at these times.

4.3. Implications for Past South Atlantic Deepwater Circulation

The past AABW end-member δ^{13}C composition is not well known due to scarce data in the water formation regions around Antarctica [e.g., *Marchitto and Broecker*, 2006]. Thus, many South Atlantic LGM studies use δ^{13}C minimum values (~0.9‰) from the deep southern Cape Basin and adjacent areas as most probable AABW end-member analogues [*Curry and Oppo*, 2005; *Mackensen*, 2001; *Martínez-Méndez et al.*, 2009; *Ninnemann and Charles*, 2002]. During the LGM, these deep SE Atlantic δ^{13}C values were far lower than the SE Pacific δ^{13}C values from the East Pacific Rise area [*Ninnemann and Charles*, 2002] (Figure 6). For instance, during the LGM an invasion of very low δ^{13}C AABW at the expense of current CDW is indicated, while the missing difference during the MIS 8 glaciation implies either that no AABW invasion occurred at that time or that AABW end-member δ^{13}C composition was undistinguishable from CDW (i.e., AABW was the dominant constituent determining CDW δ^{13}C). LGM studies often link the occurrence of the extremely depleted benthic δ^{13}C values in the southern Cape Basin to changes in the expansion and formation mechanisms of W-AABW, resulting in a drastic lowering of its end-member δ^{13}C signature [e.g., *Curry and Oppo*, 2005; *Marchitto and Broecker*, 2006; *Martínez-Méndez et al.*, 2009; *Ninnemann and Charles*, 2002]. This is evident in the negative LGM difference between records PS75/059-2 and ODP Site 1089 (Figure 6). One potential cause for the LGM δ^{13}C depletion might have been a strongly reduced air-sea gas exchange during AABW formation, related to expansion of sea ice coverage around Antarctica [*Mackensen*, 2012] Additional depletion may have occurred to the buildup of respired CO_2 in the deepest/southernmost Antarctic water masses [*Toggweiler et al.*, 2006]. Likewise for pre-LGM times, more negative δ^{13}C values for the southern Cape Basin record ODP Site 1089 may therefore point toward an increased influence of very δ^{13}C depleted AABW, and conversely, a restriction of AABW influence only to this location as it did not dominate the CDW δ^{13}C signature. If true, the difference between both records indicates very complex CDW and AABW interactions further back in time, associated with changes in past AABW end-member δ^{13}C composition (Figure 6). To the extent that ODP 1089 is depicting the true AABW end-member (pending confirmation from a site bathed more directly by AABW), AABW-CDW differences then provide a monitor of the relative contribution (and dominance) of AABW in the common CDW composition. The current LGM picture with the exceptionally low benthic δ^{13}C values in the southernmost South Atlantic relative to CDW bathed sites, indicating particularly strong AABW influence only at this location, appears to be not a simple or systematic feature of other glacial stages. Indeed, the persistent Pacific-derived CDW presence in the northern Cape Basin (Figure 5) indicates that the propagation of low- δ^{13}C Antarctic-sourced bottom waters was restricted and did not reach into the lower latitude Atlantic, thus limiting the volumetric importance of bottom waters bathing the southern Cape Basin. Due to its characteristic δ^{18}O and δ^{13}C composition, deep southern Cape Basin waters may represent an individual glacial W-AABW variety, or more pure end-member, during the LGM, distinct to a much lesser δ^{13}C depleted glacial AABW, which flowed into the Atlantic interior along its western boundary [*Hoffman and Lund*, 2012; *Martínez-Méndez et al.*, 2009].

As total AABW production may have been higher during glacial times [e.g., *Adkins*, 2013], this glacial W-AABW variety was only a relatively smaller component of glacial Southern-Sourced Deepwater Masses that propagated into the lower latitude deep Southeast Atlantic; via its mixing into CDW. According to our comparisons it seems unlikely that W-AABW in its undiluted form was exported directly further north toward the equatorial Atlantic direction, at least during the LGM. Such enhanced transport would have only been possible if restrictions by seafloor topography on dense AABW flow could have been overcome through a vertical expansion of AABW at the expense of glacial Northern Atlantic Deepwater distribution. Otherwise, as today, the densest varieties of Antarctic bottom water will continue to be constrained by topography with only lighter, mixed versions flowing northward filling basins. However, Atlantic-wide highest published LGM δ^{18}O values, obtained from the Brazil margin, indicate that during the LGM AABW penetrated along the western boundary far northward into the Atlantic interior [*Hoffman and Lund*, 2012]. This northward flowing AABW appears distinct in $\delta^{18}O$ and $\delta^{13}C$ space from that occupying the SE Atlantic [*Hoffman and Lund*, 2012] but its isotopic composition is much to the "common" CDW composition.

5. Conclusions

In this study we examined the deepwater exchange between the Pacific and Atlantic basins over the past 500 ka. Using benthic foraminiferal $\delta^{13}C$ data from the East Pacific Rise, we characterized the $\delta^{13}C$ composition of SE Pacific CDW, prior to its transition trough the Drake Passage, and showed that it closely co-evolved with the CDW composition in the deep SE Atlantic, northern Cape Basin. Our results imply a continuous deepwater exchange between the SE Pacific and SE Atlantic throughout the past 500 ka. We conclude that a common CDW was maintained between the SE Pacific and the SE Atlantic (Northern Cape Basin). In contrast, our comparison to the southern Cape Basin records indicates that an interbasin $\delta^{13}C$ gradient was particularly pronounced during the LGM and occurred in weaker form during most of the other glaciations but was absent or even positive during MIS 8.

Our results confirm that deep waters in the southernmost areas of the SE Atlantic, including the southern Cape Basin, evolved differently from a CDW that occupied the deepwater layer in the SE Pacific and the SE Atlantic, as proposed previously [*Ninnemann and Charles*, 2002]. This divergent evolution of southern South Atlantic deep waters can be explained by repeated northward expansion of W-AABW into that area, combined with changes in its end-member $\delta^{13}C$ signature. Thus, defining CDW as an individual deepwater mass in the Atlantic reveals a more differentiated picture on past AABW extent. In that regard, the current LGM picture associated with the extremely low LGM benthic $\delta^{13}C$ values in the southernmost SE Atlantic needs to be refined. Such differentiations in South Atlantic deepwater characteristics might be helpful when discussing past deep Southern Ocean water mass signatures and end-member compositions as well as when quantifying their contribution to global deep water and atmospheric CO_2 changes on glacial-interglacial time scales.

Acknowledgments
We thank the captain, crew, and scientific party of R/V *Polarstern* for their support during the ANT-XXVI-2 cruise. We thank A. Mackensen for discussions and S. Steph for providing unpublished isotope data and for supporting the isotope measurements. U. Bock, G. Meier, and L. Schönborn provided technical support at the Alfred Wegener Institute. G. Martínez-Méndez, J. Collins, C. Lange, and S. Romahn provided valuable comments and suggestions that helped to improve the manuscript. M. Menzel assisted in software questions. This work is a contribution to the PACES II research program and was financially supported by the Alfred-Wegener-Institut Helmholtz-Zentrum für Polar- und Meeresforschung. The data reported in this manuscript are available online in the PANGAEA data repository (https://doi.pangaea.de/10.1594/PANGAEA.833422).

References

Adkins, J. F. (2013), The role of deep ocean circulation in setting glacial climates, *Paleoceanography*, *28*, 539–561, doi:10.1002/palo.20046.

Broecker, W. S., and E. Maier-Reimer (1992), The influence of air and sea exchange on the carbon isotope distribution in the sea, *Global Biogeochem. Cycles*, *6*, 315–320, doi:10.1029/92GB01672.

Broecker, W. S., et al. (1998), How much deep water is formed in the Southern Ocean?, *J. Geophys. Res.*, *103*, 15,833–15,843, doi:10.1029/98JC00248.

Curry, W. B., and D. W. Oppo (2005), Glacial water mass geometry and the distribution of $\delta^{13}C$ of ΣCO_2 in the western Atlantic Ocean, *Paleoceanography*, *20*, PA1017, doi:10.1029/2004PA001021.

Curry, W. B., J. C. Duplessy, L. D. Labeyrie, and N. J. Shackleton (1988), Changes in the distribution of $\delta^{13}C$ of deep water ΣCO_2 between the last glaciation and the Holocene, *Paleoceanography*, *3*, 317–341, doi:10.1029/PA003i003p00317.

Duplessy, J. C., N. J. Shackleton, R. G. Fairbanks, L. Labeyrie, D. Oppo, and N. Kallel (1988), Deepwater source variations during the last climatic cycle and their impact on the global deepwater circulation, *Paleoceanography*, *3*, 343–360, doi:10.1029/PA003i003p00343.

Duplessy, J.-C., N. J. Shackleton, R. K. Matthews, W. Prell, W. F. Ruddiman, M. Caralp, and C. H. Hendy (1984), ^{13}C Record of benthic foraminifera in the last interglacial ocean: Implications for the carbon cycle and the global deep water circulation, *Quat. Res.*, *21*, 225–243.

Garcia, H. E., R. A. Locarnini, T. P. Boyer, J. I. Antonov, M. M. Zweng, and O. K. Baranova (2010a), World Ocean Atlas 2009, Volume 4: Nutrients (phosphate, nitrate, silicate), in *NOAA Atlas NESDIS 71*, edited by S. Levitus, 398 pp., U.S. Gov. Print. Off., Washington, D. C.

Garcia, H. E., R. A. Locarnini, T. P. Boyer, J. I. Antonov, O. K. Baranova, M. M. Zweng, and D. R. Johnson (2010b), World Ocean Atlas 2009, Volume 3: Dissolved oxygen, apparent oxygen utilization, and oxygen saturation, in *NOAA Atlas NESDIS 70*, edited by S. Levitus, 344 pp., U.S. Gov. Print. Off., Washington, D. C.

Gebbie, G. (2014), How much did Glacial North Atlantic Water shoal?, *Paleoceanography*, *29*, 190–209, doi:10.1002/2013PA002557.

Gersonde, R. (2011), The expedition of the research vessel "Polarstern" to the polar South Pacific in 2009/2010 (ANT-XXVI/2 - BIPOMAC), *Berichte zur Polar- und Meeresforschung (Rep. Polar Marine Res.)*, *632*, 330.

Hesse, T., M. Butzin, T. Bickert, and G. Lohmann (2011), A model-data comparison of δ13C in the glacial Atlantic Ocean, *Paleoceanography*, *26*, PA3220, doi:10.1029/2010PA002085.

Hodell, D. A., C. D. Charles, and U. S. Ninnemann (2000), Comparison of interglacial stages in the South Atlantic sector of the Southern Ocean for the past 450 kyr: Implifications for Marine Isotope Stage (MIS) 11, *Global Planet. Change*, *24*(1), 7–26.

Hodell, D. A., C. D. Charles, and F. J. Sierro (2001), Late Pleistocene evolution of the ocean's carbonate system, *Earth Planet. Sci. Lett.*, *192*(2), 109–124.

Hodell, D. A., K. A. Venz, C. D. Charles, and U. S. Ninnemann (2003a), Pleistocene vertical carbon isotope and carbonate gradients in the South Atlantic sector of the Southern Ocean, *Geochem. Geophys. Geosyst.*, *4*(1), 1004, doi:10.1029/2002GC000367.

Hodell, D. A., C. D. Charles, J. H. Curtis, P. G. Mortyn, U. S. Ninnemann, and K. A. Venz (2003b), Data report: Oxygen isotope stratigraphy of ODP Leg 177 Sites 1088, 1089, 1090, 1093, and 1094, 1–26 pp.

Hoffman, J. L., and D. C. Lund (2012), Refining the stable isotope budget for Antarctic Bottom Water: New foraminiferal data from the abyssal southwest Atlantic, *Paleoceanography*, *27*, PA1213, doi:10.1029/2011PA002216.

Johnson, G. C. (2008), Quantifying Antarctic Bottom Water and North Atlantic Deep Water volumes, *J. Geophys. Res.*, *113*, C05027, doi:10.1029/2007JC004477.

Key, R. M., A. Kozyr, C. L. Sabine, K. Lee, R. Wanninkhof, J. L. Bullister, R. A. Feely, F. J. Millero, C. Mordy, and T. H. Peng (2004), A global ocean carbon climatology: Results from Global Data Analysis Project (GLODAP), *Global Biogeochem. Cycles*, *18*, GB4031, doi:10.1029/2004GB002247.

Kroopnick, P. M. (1985), The distribution of ^{13}C of ΣCO_2 in the world oceans, *Deep Sea Res., Part A*, *32*(1), 57–84.

Lamy, F., R. Gersonde, G. Winckler, O. Esper, A. Jaeschke, G. Kuhn, J. Ullermann, A. Martinez-Garcia, F. Lambert, and R. Kilian (2014), Increased dust deposition in the Pacific Southern Ocean during glacial periods, *Science*, *343*(6169), 403–407.

Lisiecki, L. E., and P. A. Lisiecki (2002), Application of dynamic programming to the correlation of paleoclimate records, *Paleoceanography*, *17*(4), 1049, doi:10.1029/2001PA000733.

Lisiecki, L. E., and M. E. Raymo (2005), A Pliocene-Pleistocene stack of 57 globally distributed benthic δ^{18}O records, *Paleoceanography*, *20*, PA1003, doi:10.1029/2004PA001071.

Lund, D. C., J. F. Adkins, and R. Ferrari (2011), Abyssal Atlantic circulation during the Last Glacial Maximum: Constraining the ratio between transport and vertical mixing, *Paleoceanography*, *26*, PA1213, doi:10.1029/2010PA001938.

Lüthi, D., et al. (2008), High resolution carbon dioxide concentration record 650,000-800,000 years before present, *Nature*, *453*(7193), 379–382.

Lynch-Stieglitz, J. (2003), Tracers of past ocean circulation, in *Treatise on Geochemistry (volume ed. H. Elderfield)*, edited by H. D. Holland and K. K. Turekian, pp. 433–451, Elsevier-Pergamon, Oxford.

Mackensen, A. (2001), Oxygen and carbon stable isotope tracers of Weddell Sea water masses: New data and some paleoceanographic implications, *Deep Sea Res., Part I*, *48*(6), 1401–1422.

Mackensen, A. (2012), Strong thermodynamic imprint on recent bottom water and epibenthic δ^{13}C in the Weddell Sea revealed: Implications for glacial Southern Ocean ventilation, *Earth Planet. Sci. Lett.*, *317–318*, 20–26.

Mackensen, A., H. W. Hubberten, T. Bickert, G. Fischer, and D. K. Futterer (1993), The δ^{13}C in benthic foraminiferal tests of *Fontbotia Wuellerstorfi* (Schwager) relative to the δ^{13}C of dissolved inorganic carbon in Southern Ocean deep water: Implications for glacial ocean circulation models, *Paleoceanography*, *8*, 587–610, doi:10.1029/93PA01291.

Mackensen, A., M. Rudolph, and G. Kuhn (2001), Late Pleistocene deep-water circulation in the subantarctic eastern Atlantic, *Global Planet. Change*, *30*(3–4), 197–229.

Marchitto, T. M., and W. S. Broecker (2006), Deep water mass geometry in the glacial Atlantic Ocean: A review of constraints from the paleonutrient proxy Cd/Ca, *Geochem. Geophys. Geosyst.*, *7*, Q12003, doi:10.1029/2006GC001323.

Martínez-Méndez, G., E. G. Molyneux, I. R. Hall, and R. Zahn (2009), Variable water column structure of the South Atlantic on glacial-interglacial time scales, *Quat. Sci. Rev.*, *28*(27–28), 3379–3387.

Martínez-Méndez, G., D. Hebbeln, M. Mohtadi, F. Lamy, R. De Pol-Holz, D. Reyes-Macaya, and T. Freudenthal (2013), Changes in the advection of Antarctic Intermediate Water to the northern Chilean coast during the last 970 kyr, *Paleoceanography*, *28*, 607–618, doi:10.1002/palo.20047.

Matsumoto, K., and J. Lynch-Stieglitz (1999), Similar glacial and Holocene deep water circulation inferred from southeast Pacific benthic foraminiferal carbon isotope composition, *Paleoceanography*, *14*, 149–163, doi:10.1029/1998PA900028.

Naveira Garabato, A. C., K. J. Heywood, and D. P. Stevens (2002), Modification and pathways of Southern Ocean Deep Waters in the Scotia Sea, *Deep-Sea Res. Part I-Oceanogr. Res. Pap.*, *49*(4), 681–705.

Naveira Garabato, A. C., D. P. Stevens, A. J. Watson, and W. Roether (2007), Short-circuiting of the overturning circulation in the Antarctic Circumpolar Current, *Nature*, *447*(7141), 194–197.

Ninnemann, U. S., and C. D. Charles (2002), Changes in the mode of Southern Ocean circulation over the last glacial cycle revealed by foraminiferal stable isotopic variability, *Earth Planet. Sci. Lett.*, *201*(2), 383–396.

Oppo, D. W., and R. G. Fairbanks (1987), Variability in the deep and intermediate water circulation of the Atlantic Ocean during the past 25,000 years: Northern Hemisphere modulation of the Southern Ocean, *Earth Planet. Sci. Lett.*, *86*(1), 1–15.

Oppo, D. W., R. G. Fairbanks, A. L. Gordon, and N. J. Shackleton (1990), Late Pleistocene Southern Ocean δ^{13}C variability, *Paleoceanography*, *5*, 43–54, doi:10.1029/PA005i001p00043.

Orsi, A. H., T. Whitworth, and W. D. Nowlin (1995), On the meridional extent and fronts of the Antarctic Circumpolar Current, *Deep-Sea Res. Part I-Oceanogr. Res. Pap.*, *42*(5), 641–673.

Orsi, A. H., G. C. Johnson, and J. L. Bullister (1999), Circulation, mixing, and production of Antarctic Bottom Water, *Prog. Oceanogr.*, *43*(1), 55–109.

Orsi, A. H., W. M. Smethie, and J. L. Bullister (2002), On the total input of Antarctic waters to the deep ocean: A preliminary estimate from chlorofluorocarbon measurements, *J. Geophys. Res.*, *107*(C8), 3122, doi:10.1029/2001JC000976.

Paillard, D., L. Labeyrie, and P. Yiou (1996), Macintosh program performs time-series analysis, *Eos Trans. AGU*, *77*(39), 379, doi:10.1029/96EO00259.

Pardo, P. C., F. F. Perez, A. Velo, and M. Gilcoto (2012), Water masses distribution in the Southern Ocean: Improvement of an extended OMP (eOMP) analysis, *Prog. Oceanogr.*, *103*, 92–105.

Petit, J. R., et al. (1999), Climate and atmospheric history of the past 420,000 years from the Vostok ice core, Antarctica, *Nature*, *399*(6735), 429–436.

Piotrowski, A. M., S. L. Goldstein, S. R. Hemming, and R. G. Fairbanks (2005), Temporal relationships of carbon cycling and ocean circulation at glacial boundaries, *Science*, *307*(5717), 1933–1938.

Piotrowski, A. M., S. L. Goldstein, S. R. Hemming, R. G. Fairbanks, and D. R. Zylberberg (2008), Oscillating glacial northern and southern deep water formation from combined neodymium and carbon isotopes, *Earth Planet. Sci. Lett.*, *272*(1–2), 394–405.

Reid, J. L. (1986), On the total geostrophic circulation of the South Pacific Ocean: Flow patterns, tracers and transports, *Prog. Oceanogr.*, *16*(1), 1–61.

Reid, J. L. (1989), On the total geostrophic circulation of the South Atlantic Ocean: Flow patterns, tracers, and transports, *Prog. Oceanogr.*, *23*(3), 149–244.

Schlitzer, R.. (2012), Ocean data view. [Available at http://odv.awi.de.]

Skinner, L. C. (2009), Glacial-interglacial atmospheric CO_2 change: A possible "standing volume" effect on deep-ocean carbon sequestration, *Clim. Past*, *5*, 537–550, doi:10.5194/cp-5-537-2009.

Toggweiler, J. R. (1999), Variation of atmospheric CO_2 by ventilation of the ocean's deepest water, *Paleoceanography*, *14*, 571–588, doi:10.1029/1999PA900033.

Toggweiler, J. R., J. L. Rusell, and S. R. Carson (2006), Midlatitude westerlies, atmospheric CO2, and climate change during ice ages, *Paleoceanography*, *21*, PA2005, doi:10.1029/2005PA001154.
Venz, K. A., and D. A. Hodell (2002), New evidence for changes in Plio-Pleistocene deep water circulation from Southern Ocean ODP Leg 177 Site 1090, *Palaeogeogr. Palaeoclimatol. Palaeoecol.*, *182*(3–4), 197–220.
Wunsch, C. (2003), Determining paleoceanographic circulations, with emphasis on the Last Glacial Maximum, *Quat. Sci. Rev.*, *22*, 371–385.